Acta Cryst. (1985). B41, 5-11

Crystal Chemistry and Structure of Na_2SO_4(I) and Its Solid Solutions*

BY W. EYSEL

Mineralogisch-Petrographisches Institut der Universität, D-6900 Heidelberg, Federal Republic of Germany

AND H. H. HÖFER, K. L. KEESTER† AND TH. HAHN

Institut für Kristallographie der Technischen Hochschule, D-5100 Aachen, Federal Republic of Germany

(*Received* 12 *September* 1983; *accepted* 24 *July* 1984)

Abstract

In the high-temperature polymorph Na_2SO_4(I) up to 30% cation vacancies can be generated by substitution of Na^+ by bi- and trivalent ions. Phase diagrams and lattice parameters of these solid solutions are presented. The hexagonal high-temperature form and its monoclinic distortions can be quenched to room temperature. A structure determination was carried out. Structural and experimental data are: $P6_3/mmc$, $a = 5{\cdot}326\ (2)$, $c = 7{\cdot}126\ (3)$ Å, $V = 175{\cdot}06$ Å^3, $Z = 2$, $D_x = 2{\cdot}695$ Mg m^{-3}, λ(Ag $K\alpha$) = 0·55936 Å, $R = 0{\cdot}09$ for 165 reflections. The crystal structure is characterized by strong orientational disorder of the SO_4 tetrahedra. The disorder, aliovalent solid solutions, thermal expansion and ionic conductivity are discussed.

Introduction

Na_2SO_4 has four well established modifications and a rather complicated transition behavior, which is discussed elsewhere (Mehrotra, Hahn, Eysel & Arnold, 1984). The following phase transitions occur:

$$(V) \xleftrightarrow{473\ K} (III) \xleftrightarrow{503\ K} (II) \xleftrightarrow{510\ K} (I) \xleftrightarrow{1156\ K} \text{Liquid}.$$

In the present paper only the hexagonal high-temperature form, Na_2SO_4(I), is of interest. It transforms spontaneously and reversibly into the structurally related polymorph Na_2SO_4(II). As a consequence, pure Na_2SO_4(I) cannot be quenched to room temperature. Stabilization, however, is possible with various solid solutions.

Na_2SO_4(I) is particularly flexible in forming solid solutions: Na^+ ($r = 1{\cdot}0$ Å) can be completely replaced by the much larger K^+ (1·3 Å) (Eysel, 1973) and to a large extent by aliovalent ions M^{2+} and M^{3+}. In addition, unlimited substitution of the SO_4 tetrahedra by the much smaller planar CO_3 triangles is known (Mehrotra, 1973). Also, combined substitutions, M^{3+} for Na^+ and CO_3^{2-} for SO_4^{2-}, have been synthesized (Schubert & Eysel, 1980).

In this paper the substitution of Na^+ by bi- and trivalent ions, resulting in high cation-vacancy concentrations, is reported. The pronounced ionic conductivity based on these vacancies has been described by Höfer, Eysel & von Alpen (1981).

The structure type of Na_2SO_4(I) is the high-temperature structure of many $A_2[BX_4]$ compounds. Several structure proposals and determinations have been described but an unambiguous result is still missing. This is mainly due to a lack of suitable single crystals and the occurrence of disorder phenomena. As a contribution to this problem a structure determination, using a stabilized single crystal of Na_2SO_4(I), is reported.

Experimental

Powder samples were prepared from analytical-grade sulfates (Merck, Koch-Light) which were melted for a few minutes in Pt crucibles and quenched in air. Investigations were performed with a Norelco powder diffractometer and a high-temperature Guinier camera. For the determination of the phase diagrams annealing experiments at various subsolidus temperatures were carried out. The single crystals for the structure determination were obtained by slowly cooling a sample of composition $(Na_{0{\cdot}94}Y_{0{\cdot}02}\square_{0{\cdot}04})_2SO_4$ ($\square$ = vacancy) from the melt down to 600 K and subsequently quenching. The crystals contained 1·2 mol% $Y_2(SO_4)_3$ which is the minimal amount that stabilizes form (I). Crystal dimensions $0{\cdot}136 \times 0{\cdot}153 \times 0{\cdot}340$ mm.

Data collection: automatic single-crystal diffractometer (AED, Siemens); Ag $K\alpha$ radiation (λ = 0·55936 Å); lattice parameters refined from powder diffractometer data; 1200 reflections up to $2\theta = 53°$, with $-2 \le h \le 8$, $-2 \le k \le 9$, $-2 \le l \le 11$; 216 independent reflections, 165 with $|F_o| > 2\sigma(F_o)$; $F(000) = 140$; Lorentz and polarization corrections, no absorption or extinction corrections. Measurements of the

* Presented at the Tenth and Eleventh International Congresses of the International Union of Crystallography held in Amsterdam (Keester, Eysel & Hahn, 1975) and Warsaw (Höfer, von Alpen & Eysel, 1978), respectively.

† Present address: Exxon Enterprises, 3099 Orchard Drive, San José, CA 95134, USA.

0108-7681/85/010005-07$01.50

standard reflection $\bar{2}\bar{2}\bar{2}$ at regular intervals showed deviations with time of less than 2% in intensity. There was an unusual decrease of intensities with $\sin\theta/\lambda$. Fourier and full-matrix least-squares refinements [using F_o and weights $1/\sigma(F_o)$] were performed with the *XRAY* system of crystallographic programs (Stewart, Kruger, Ammon, Dickinson & Hall, 1972).* Atomic scattering factors for neutral atoms Na, S and O were taken from *International Tables for X-ray Crystallography* (1974). The results were reproduced with a second crystal measured on another single-crystal diffractometer (CAD-4, Nonius).

Solid solutions of Na_2SO_4(I)

The phase diagrams of many Na_2SO_4-$M^{2+}SO_4$ (M^{2+} = Mg, Ni, Zn, Cd, Ca, Pb, Ba, *etc.*) systems have been described, and extended solid-solution series for Na_2SO_4(I) have been reported (Table 1). For several systems the results were confirmed by reinvestigation. As an example, the phase diagram of the system Na_2SO_4-$NiSO_4$ is shown in Fig. 1. Surprisingly, Na_2SO_4(I) also forms solid solutions in Na_2SO_4-$M_2^{3+}(SO_4)_3$ systems (Table 1). Fig. 2 shows the Na_2SO_4-rich part of the system Na_2SO_4-$Y_2^{3+}(SO_4)_3$.

Even though these aliovalent substitutions have been known since about 1910 (see references in Table 1), the structural background has never been discussed. Crystal-chemical reasons suggest the substitution types $2Na^{2+} = 1M^{2+} + 1\square$ and $3Na^{+} = 1M^{3+} + 2\square$, corresponding to the formulae $Na_{2-2x}M_x^{2+}\square_xSO_4$ and $Na_{2-2x}M_{2x/3}^{3+}\square_{4x/3}SO_4$, which were confirmed indirectly by the results of ionic-conductivity measurements (Höfer, Eysel & von Alpen, 1981). Up to about 30% cation vacancies can be generated in the Na_2SO_4(I) structure.

With increasing amounts of M^{2+} and M^{3+} ions the X-ray powder diffraction peaks become broader, indicating decreasing perfection. On cooling *pure* Na_2SO_4, the transition sequence Na_2SO_4(I)→ Na_2SO_4(II)→ Na_2SO_4(III) is observed, with form (III) occurring at room temperature. In solid solutions, however, it is possible to quench the high-temperature form (I). The lattice parameters of quenched samples in Figs. 3 and 4 exhibit opposite slopes of a and c, with nearly constant cell volumes. The lattice parameters of pure Na_2SO_4(I) at room temperature can be extrapolated to $a = 5{\cdot}36$ Å and

Table 1. Na_2SO_4(I) *solid solutions with* $M^{2+}SO_4$ *and* $M_2^{3+}(SO_4)_3$

Substituting ion M, ionic radius (Å)	Limit of solid solution mol% $M^{2+}SO_4$ or $M_2^{3+}(SO_4)_3$	% cation vacancies	Reference†
Ni^{2+}, 0·70	25	12·5	(1), (2)
Mg^{2+}, 0·72	36	18	(3)
Cu^{2+}, 0·73	30	15	(4), (5)
Co^{2+}, 0·74	35	17·5	(1)
Zn^{2+}, 0·75	30	15	(6)
Mn^{2+}, 0·82	55	27·5	(7)
Cd^{2+}, 0·95	40	20	(8)
Ca^{2+}, 1·00	40	20	(2), (9), (10)
Sr^{2+}, 1·16	17	8·5	(2)
Pb^{2+}, 1·18	17	8·5	(11), (12)
Ba^{2+}, 1·36	21	10·5	(13)
Cr^{3+}, 0·62	>2·5		(2)
Fe^{3+}, 0·65	14	22	(5)
In^{3+}, 0·79	>2·5*		(2)
Y^{3+}, 0·89	20	29	(2)
Gd^{3+}, 0·94	>2·5*		(2)
Eu^{3+}, 0·95	>2·5*		(2)
La^{3+}, 1·06	>2·5*		(2)

* Form (I) was stabilized with 2·5 mol% of sulfates $M_2^{3+}(SO_4)_3$. The limits of solid solution are probably much higher.

† (1) Bol'shakov & Fedorov (1956). (2) This paper. (3) Ginsberg (1909). (4) Bellanca & Carapezza (1951). (5) Bol'shakov, Fedorov & Ilina (1963). (6) Evseeva (1953). (7) Calcagni & Marotta (1915). (8) Calcagni & Marotta (1913). (9) Müller (1910). (10) Bellanca (1942). (11) Calcagni & Marotta (1912). (12) Perrier & Bellanca (1940). (13) Calcagni (1912).

* A list of structure factors has been deposited with the British Library Lending Division as Supplementary Publication No. SUP 39504 (6 pp.). Copies may be obtained through The Executive Secretary, International Union of Crystallography, 5 Abbey Square, Chester CH1 2HU, England.

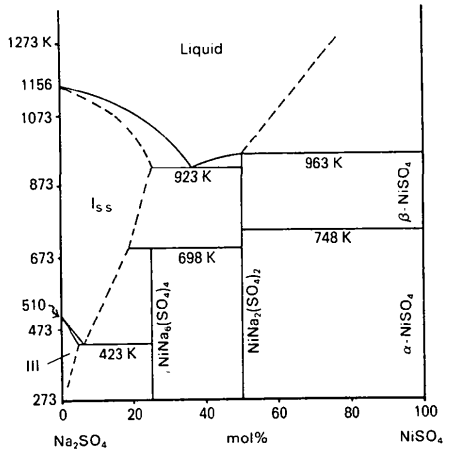

Fig. 1. Phase diagram of the system Na_2SO_4-$NiSO_4$. The very small area of Na_2SO_4(II) (s.s.) has been omitted.

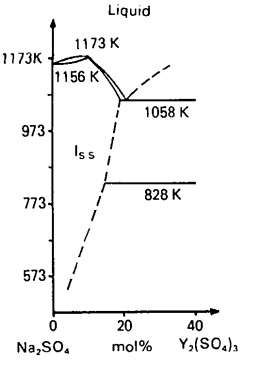

Fig. 2. Part of the phase diagram of the system Na_2SO_4-$Y_2(SO_4)_3$.

Table 2. *Lattice parameters of quenched* Na_2SO_4(I) *solid solutions at* 293 K (*except for pure* Na_2SO_4)

(Pseudo-)orthohexagonal axes. Standard deviations ±0·01 Å for the first two and ±0·003 Å for the subsequent materials.

Composition	Symmetry	a(Å)	b(Å)	c(Å)	Angle (°)	V(Å^3)	a/b
Na_2SO_4(I), 543 K	$P6_3/mmc$	9·39	5·42	7·24		368·5	$\sqrt{3}$ = 1·7321
Na_2SO_4(I), 293 K*		9·28	5·36	7·06		351·2	$\sqrt{3}$
$Na_{1.88}Y_{0.04}\square_{0.08}SO_4$		9·225	5·326	7·126		350·1	$\sqrt{3}$
$Na_{1.61}Y_{0.13}\square_{0.26}SO_4$		9·154	5·285	7·262		351·3	$\sqrt{3}$
$Na_{1.80}Ni_{0.10}\square_{0.10}SO_4$		9·209	5·317	7·114		348·3	$\sqrt{3}$
$Na_{1.80}Sr_{0.10}\square_{0.10}SO_4$		9·273	5·354	7·175		356·2	$\sqrt{3}$
$Na_{1.60}Zn_{0.20}\square_{0.20}SO_4$		9·246	5·338	7·119		351·4	$\sqrt{3}$
$Na_{1.90}Zn_{0.05}\square_{0.05}SO_4$	Monoclinic	9·265	5·348	7·121	β = 92·37	352·5	1·7324
$Na_{1.60}Ca_{0.20}\square_{0.20}SO_4$		9·246	5·338	7·134	α = 91·37	352·1	1·7321

* Extrapolated from Figs. 3 and 4.

c = 7·06 Å (Table 2). The scales of the cation vacancies and of the lattice parameters in Figs. 3 and 4 are the same for both series. The very similar slopes of the curves show that the lattice parameters are controlled predominantly by the vacancy concentration and less by the sizes and valencies of the substituting ions. The same dependence was found for the ionic conductivity.

If the samples are cooled slowly, two different monoclinic distortions may be observed (Table 2). The type with $\beta \neq 90°$ was found for solid solutions with Zn^{2+}, Ca^{2+} and Y^{3+}. The second type with $\alpha \neq 90°$ was obtained only with high Ca^{2+} contents (>9 mol% $CaSO_4$). On heating in a high-temperature Guinier camera the latter type transformed to the former just before becoming hexagonal. Powder data of the hexagonal and the two monoclinic varieties are published in the JCPDS Powder Data File (Card Nos. 29-1290, 29-1196, 29-1291).

Disorder models

In this study for the first time Na_2SO_4(I) single crystals suitable for structure determination were available. This structure type, despite the simple chemical formula, is by no means trivial, and its rather complicated disorder has led to conflicting results in the literature.

The following structural features are common to all experimental results on Na_2SO_4(I) and isostructural compounds.

(i) Small hexagonal cell (Table 2), containing only four cations and two tetrahedra.

(ii) Simple 'basic structure' of Fig. 5; the large spheres symbolize the SO_4 tetrahedra without regard to their orientation.

(iii) Laue class $6/mmm$ and a tertiary c glide, resulting in the possible space groups $P6_3/mmc$, $P6_3mc$, and $P\bar{6}2c$. These results were confirmed in the present study.

(iv) Existence of secondary (vertical) mirror planes in the structure, thus excluding $P\bar{6}2c$.

Discrepancies among authors, however, exist with respect to the orientation of the tetrahedra. For the subsequent discussion a tetrahedron is represented by an arrow, as shown in Fig. 6(a). The direction of the arrow indicates the orientation of that tetrahedral apex which points along or nearly along the threefold

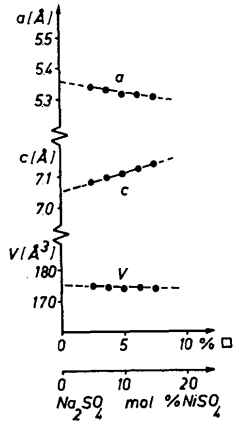

Fig. 3. Lattice parameters and cell volume of Na_2SO_4(I) solid solutions in the system Na_2SO_4–$NiSO_4$. □ = cation vacancy.

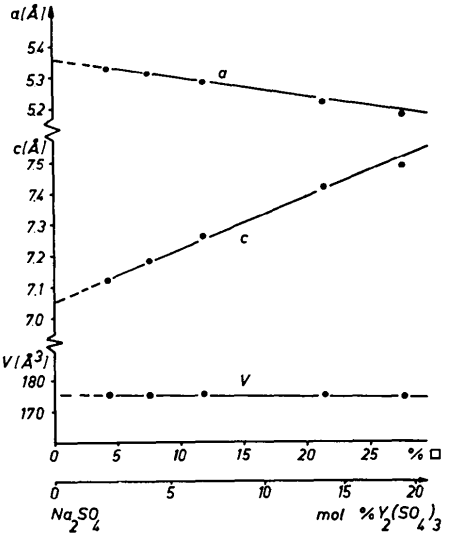

Fig. 4. Lattice parameters and cell volume of Na_2SO_4(I) solid solutions in the system Na_2SO_4–$Y_2(SO_4)_3$.

axis. Based on the ordered structure, symbolized by Fig. 6(*b*) (polar space group $P6_3mc$), several types of orientational disorder of the tetrahedra have to be considered:

(1) 'up-down' disorder,* resulting in a mirror plane perpendicular to the *c* axis (centrosymmetric space group $P6_3/mmc$, Fig. 6*c*);

(2) 'tilting' disorder due to inclination of the 'split' tetrahedra against the trigonal axis with α = tilting angle ($P6_3mc$, Fig. 6*d*);

(3) 'left-right' disorder with respect to the vertical mirror plane ($P6_3mc$ and $P6_3/mmc$, not illustrated);

(4) combination of (1) and (2) ($P6_3/mmc$, Fig. 6*e*);

(5) the tilting angle $\alpha = 31{\cdot}5°$ represents a special case for which (2) and (4) become identical, because all split tetrahedra have one edge parallel to the *c* axis ($P6_3/mmc$, Fig. 6*f*).

Most of these possibilities have been considered in the literature:

Fig. 5: Bredig (1943) for Na_2SO_4 and K_2SO_4, rotation of SO_4 groups;

Fig. 6(*b*): Eysel & Hahn (1970) for α-Ca_2SiO_4; Iwai, Sakai & Watanabe (1973) for high-K_2SO_4; Mehrotra (1973) for high-Na_2SeO_4; Kobayashi & Saito (1982) for Na_2SO_4(I);

Fig. 6(*c*): Fischmeister (1962), van den Berg & Tuinstra (1978), Miyake, Morikawa & Iwai (1980), all for high-K_2SO_4;

Fig. 6(*d*): De Wolff (1970, private communication) for high-K_2SO_4;

Fig. 6(*f*): Höfer (1979) and the present paper for Na_2SO_4(I); Arnold, Kurtz, Richter-Zinnius, Bethke & Heger (1981) for high-K_2SO_4.

In the sequel the average structure of Na_2SO_4(I) is described and an attempt is made to interpret it on the basis of the disorder models above.

* Ordered up-down arrangements occur in several related crystal structures, *e.g.* $NaK_3(SO_4)_2$ (glaserite) and low-K_2SO_4.

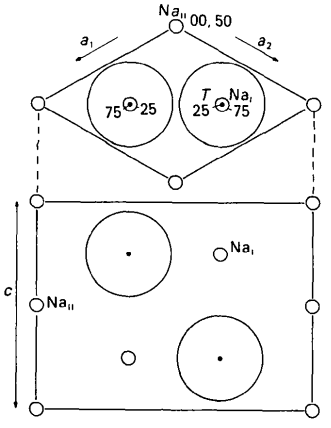

Fig. 5. 'Basic structure' for Na_2SO_4(I). Small spheres Na, large spheres SO_4 tetrahedra. Space group $P6_3/mmc$.

Structure determination

Statistical methods, such as the $N(z)$ test, allowed no distinction between space groups $P6_3mc$ and $P6_3/mmc$, nor did investigations with a second-harmonic analyzer.

Fourier computations were carried out based upon the polar models in Figs. 6(*b*) and 6(*d*) and the centrosymmetric models in Figs. 6(*c*), 6(*e*), and 6(*f*). For the noncentrosymmetric models all phases were close to 0 or π. Moreover, it turned out that for *all* models corresponding structure factors received very nearly the same phases. As a consequence, the calculated electron density is model-invariant within the accuracy of the method.

The Fourier sections $\rho(xy\frac{1}{4})$, $\rho(xy\frac{1}{15})$, and $\rho(\bar{x}xz)$ are shown in Figs. 7 and 8. The most remarkable result is the fact that the centers of the S and of three O maxima are located on the same level $z = \frac{1}{4}$, simulating a planar SO_3 group. In $\rho(xy\frac{1}{4})$ the S maxima are circular whereas the O contours show a slight elongation normal to the S–O direction. In $\rho(xy\frac{1}{15})$, *i.e.* 1·3 Å from $z = \frac{1}{4}$, the S atom has vanished but the O atoms are still visible. This is also evident from $\rho(\bar{x}xz)$ which, in addition, shows a peculiar banana-shaped distribution of the O density. The S atom is slightly elongated along the *c* axis (non-equidistant contours in Fig. 8 simulate a stronger elongation). No electron density at all is found on the trigonal axis above and below the S atom. This excludes the disorder models in Figs. 6(*b*) and 6(*c*).

The observed electron density was interpreted by fitting regular SO_4 tetrahedra with S–O distances of 1·47 Å. The only agreement was obtained for the model of Fig. 6(*f*) with the special tilting angle α = 31·50°. For this angle the 'upper' and 'lower' member of each pair of tetrahedra in Fig. 6(*e*) merge and the population parameter (p.p.) is increased to $\frac{1}{3}$. The

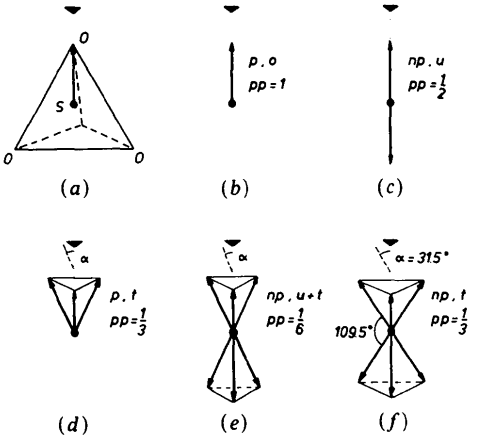

Fig. 6. Representation of possible tetrahedral orientations in the structure of Na_2SO_4(I) by arrows; *p* polar, *np* non-polar, *o* ordered, *u* up-down disorder, *t* tilting disorder, *pp* population parameter.

resulting arrangement is shown in Fig. 9. It consists of three superimposed split tetrahedra, each with one edge parallel and one perpendicular to the c axis. In Figs. 7 and 8 the O and S positions of the model are marked by crosses; the three split tetrahedra are designated A, B, and C. The close agreement between the Fourier maxima and the crosses proves the correctness of the proposed structure, as do the rather flat features in the final difference Fourier svnthesis.

Numerous full-matrix least-squares refinements were carried out, varying the positional parameters defined by the different models, as well as isotropic temperature factors of all atoms. This resulted in a weighted R factor $R_w = 0{\cdot}093$ which is higher than usual owing to the strong disorder. The continuous electron density of the O atoms, however, precludes a meaningful refinement of individual atomic positions and bond lengths. Indeed, the least-squares calculations did not lead to a significant and chemically reasonable improvement of the structure; instead, high temperature factors resulted. For this reason, in Table 3 the positional parameters derived from the model (without standard deviations) are listed; the isotropic temperature factors B were obtained from the least-squares calculations.

The above interpretation of the observed electron density is supported by the following facts.

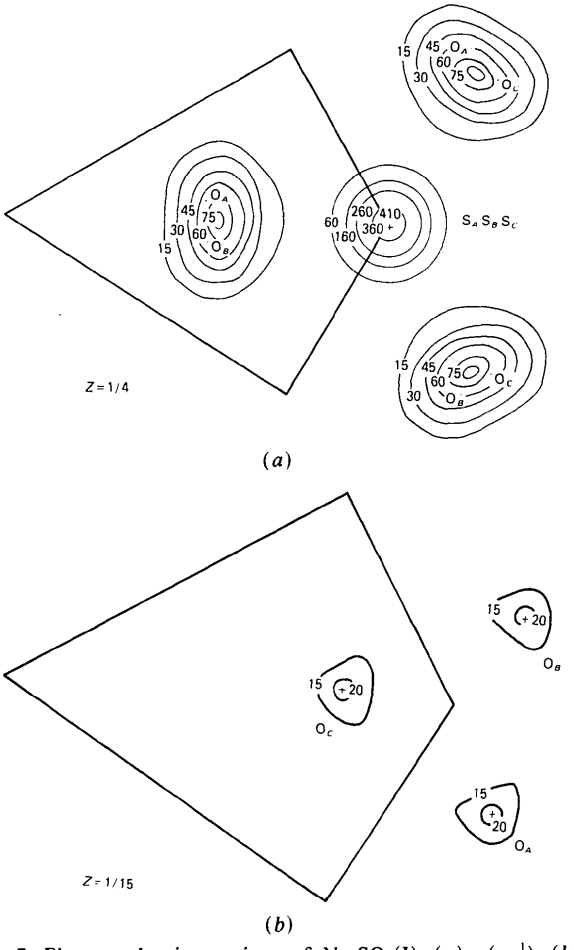

Fig. 7. Electron density sections of Na_2SO_4(I). (*a*) $\rho(xy\frac{1}{4})$, (*b*) $\rho(xy\frac{1}{15})$. The three equivalent tetrahedra are designated A, B, and C. An asymmetric unit is outlined. Crosses are atomic positions of the model in Fig. 6(*f*).

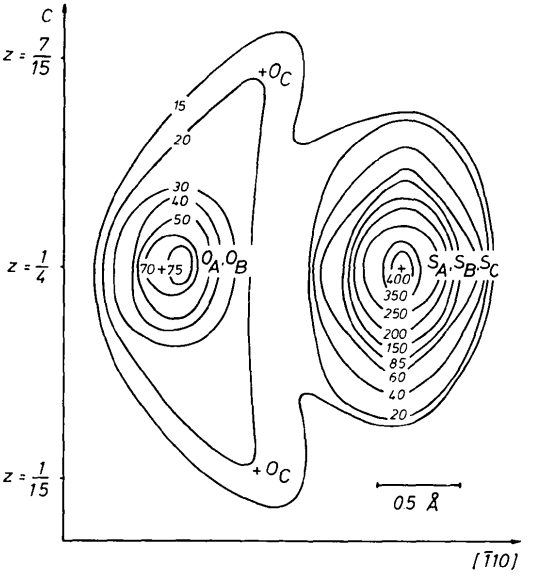

Fig. 8. Electron density section $\rho(\bar{x}xz)$ of Na_2SO_4(I). The three equivalent tetrahedra are designated A, B and C. Note that the contours of the S peak are not equidistant. Crosses are atomic positions of the model in Fig. 6(*f*).

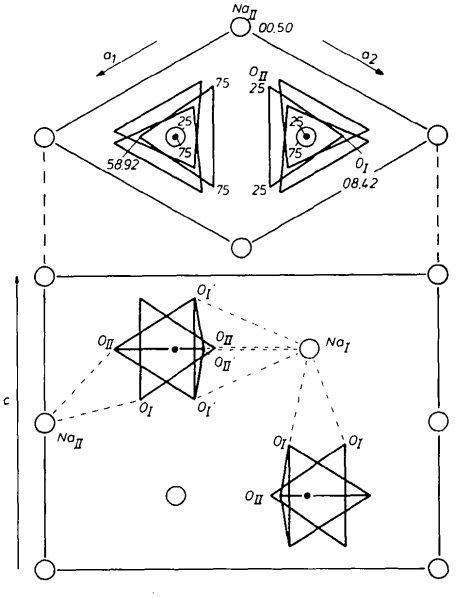

Fig. 9. Interpretation of the average structure of Na_2SO_4(I) in terms of the orientational disorder of the tetrahedra. Some representative Na–O bonds are indicated by dashed lines. The remaining bonds are obtained by applying the symmetry operations of space group $P6_3/mmc$. The O atoms are labeled as in Table 3.

Table 3. *Positional parameters (see text) and isotropic temperature factors in* Na_2SO_4(I)

Ideal SO_4 tetrahedra with d(S–O) = 1·47 Å are assumed.

	Multiplicity, Wyckoff letter	x	y	z	B(Å^2)
Na_I	2 d	$\frac{1}{3}$	$\frac{2}{3}$	$\frac{3}{4}$	6·2 (2)
Na_{II}	2 a	0	0	0	3·3 (1)
S	2 c	$\frac{1}{3}$	$\frac{2}{3}$	$\frac{1}{4}$	4·5 (2)
O_I	12 k	0·242	0·484	0·418	9·1 (3)
O_{II}	12 j	0·199	0·346	$\frac{1}{4}$	4·8 (2)

(*a*) It is the only model which explains the coplanar arrangement of the S and O_{II} maxima in Figs. 7(*a*) and 8.

(*b*) The rather sharp S maximum proves that the centers of the three split tetrahedra very nearly coincide.

(*c*) The three (elongated) O maxima in $\rho(xy\frac{1}{4})$ represent six O atoms, two from each of the three split tetrahedra *A*, *B*, and *C* (*cf.* upper part of Fig. 9).

(*d*) The remaining six O atoms of the model are located above and below the mirror plane, at about $z = \frac{1}{15}$ and $\frac{7}{15}$. They form the upper and lower part of the 'banana' in Fig. 8 and are visible as small peaks in Fig. 7(*b*) (*cf.* lower part of Fig. 9). The low electron density at the positions of these atoms, however, is unsatisfactory and a weakness of the model.

(*e*) No significant indication for disorder of the Na atoms was observed.

Because of the disorder no individual Na coordination polyhedra can be defined. The average coordinations of the two Na atoms (obtained by reducing the Na–O bonds to unit weight), are quite different: Na_I has four close (2·52 Å), two intermediate (2·80 Å), and four rather distant (3·00 Å) O neighbors. In contrast, Na_{II} is surrounded by six close and rather equidistant O atoms (2·31–2·40 Å).

Discussion

From the previous section it is evident that the feature characterizing the Na_2SO_4(I) structure is a strong positional disorder of the SO_4 tetrahedra. Whereas the Na and S atoms are rather well resolved, for the O atoms this is true only in the horizontal xy plane; in the vertical $\bar{x}xz$ plane, however, the O atoms are not resolved at all. The methods employed so far do not allow a distinction between dynamic or static (frozen-in high-temperature equilibria) disorder; 'normal' anisotropic thermal motion, however, can be excluded, both because of the unusually large disorder effect and because the measurements were made at room temperature on quenched metastable crystals. (Unfortunately, the search for domains with an electron microscope failed owing to vaporization of the sample.) The split model in Figs. 6(*f*) and 9 with its well defined atomic positions, therefore, must be considered as a limiting case upon which further 'continuous' (positional or thermal) disorder of the tetrahedra around the S atoms is superimposed. At higher temperatures certainly the thermal component will gain in importance.

Even though the crystals investigated are metastable at room temperature and contain small amounts of Y atoms, as well as cation vacancies, the authors believe that the proposed structure represents the average high-temperature state in the stability range of form (I) (above 510 K). Comparison with high-temperature powder and single-crystal patterns of pure Na_2SO_4(I) revealed no differences.

The increase in thermal motion with temperature will result in an elongation of the banana which may lead to a participation of the 'up–down disorder' in Fig. 6(*c*). This strong c component of the thermal motion is reflected in the extraordinary anisotropy of the thermal expansion of Na_2SO_4(I) which in the **c** direction is two to three orders of magnitude larger than in the **a** direction.

The tetrahedral disorder is also probably the reason for the unusual unlimited SO_4–CO_3 substitution in Na_2SO_4(I). Moreover, the variety of local cation coordinations favors the aliovalent cation substitution. For the structurally related ordered polymorphs Na_2SO_4(II) and Na_2SO_4(III) no comparable solid solutions were found.

It should be noted that the tetrahedral disorder is not the only reason for the unusual ionic conductivity, since Na_2SO_4(I) becomes a fast ionic conductor only if extrinsic cation vacancies are introduced by aliovalent substitution. Owing to oscillation of the tetrahedra the Na^+ ions can easily move from vacancy to vacancy. Thus, dynamic disorder seems more compatible with the ionic conductivity than static disorder.

It is gratifying that a similar disorder type was found for high-K_2SO_4 at 847 and 913 K by Arnold, Kurtz, Richter-Zinnius, Bethke & Heger (1981), using single-crystal neutron diffraction, and at 1073 K, by Miyake, Morikawa & Iwai (1980) with single-crystal X-ray diffraction. Density maps comparable to those in this study were found and interpreted by Arnold *et al.* in favor of the 'edge' model (Fig. 6*f*) with a small contribution of the 'apex' model (Fig. 6*c*), whereas Miyake *et al.* found only the apex model at 1073 K. Thus the three studies, even through differing in detail, strongly support each other and show that the tetrahedral disorder is not a feature of the particular compounds but rather of the whole structure type. With increasing temperature the 'up–down disorder' (Fig. 6*c*) probably strongly gains in importance.

The high-temperature forms of a large number of $M_2[TX_4]$ compounds are considered to be isostructural with Na_2SO_4(I). The assignment is usually based on high-temperature powder diagrams. It must be noted, however, that different kinds of disorder which

are based on subgroups of $P6_3/mmc$ result in very similar powder patterns. This applies in particular to the disorder types in Fig. 6.

The authors are indebted to the Deutsche Forschungsgemeinschaft and the Heinrich-Hertz-Stiftung for support of this work. Second-harmonic-generator investigations by T. Cline and W. Schulze (Pennsylvania State University) and electron-microscopic studies by Dr Köster (Ruhr University, Bochum) are gratefully acknowledged.

References

ARNOLD, H., KURTZ, W., RICHTER-ZINNIUS, A., BETHKE, J. & HEGER, G. (1981). *Acta Cryst.* B**37**, 1643-1651.
BELLANCA, A. (1942). *Period. Mineral.* **13**, 21-86.
BELLANCA, A. & CARAPEZZA, M. (1951). *Period. Mineral.* **20**, 271-307.
BERG, A. J. VAN DEN & TUINSTRA, F. (1978). *Acta Cryst.* B**34**, 3177-3181.
BOL'SHAKOV, K. A. & FEDOROV, P. I. (1956). *J. Gen. Chem. USSR*, **26**, 348-350.
BOL'SHAKOV, K. A., FEDOROV, P. I. & ILINA, N. I. (1963). *Russ. J. Inorg. Chem.* **8**, 1350-1352.
BREDIG, M. A. (1943). *J. Phys. Chem.* **47**, 587-590.
CALCAGNI, G. (1912). *Gazz. Chim. Ital.* **42**, 652-660.
CALCAGNI, G. & MAROTTA, D. (1912). *Gazz. Chim. Ital.* **42**, 674-686.
CALCAGNI, G. & MAROTTA, D. (1913). *Atti R. Accad. Naz. Lincei Mem. Cl. Sci. Fis. Mat. Nat. Sez.* II, **22**, 377.
CALCAGNI, G. & MAROTTA, D. (1915). *Gazz. Chim. Ital.* **45**, 368-376.
EVSEEVA, N. N. (1953). *Izv. Sekt Fiz.-Khim. Anal. Inst. Obshch. Neorg. Khim. Akad. Nauk. SSSR*, **22**, 162-169.
EYSEL, W. (1973). *Am. Mineral.* **58**, 736-747.
EYSEL, W. & HAHN, TH. (1970). *Z. Kristallogr.* **131**, 322-341.
FISCHMEISTER, H. (1962). *Monatsh. Chem.* **93**, 420-434.
GINSBERG, A. S. (1909). *Z. Anorg. Chem.* **61**, 126.
HÖFER, H. H. (1979). *Ionic Conductivity and Crystal Chemistry of* Na_2SO_4(I) *Solid Solutions with Aliovalent Cation Substitution* (in German). PhD Thesis, Technische Hochschule Aachen, Federal Republic of Germany.
HÖFER, H. H., VON ALPEN, U. & EYSEL, W. (1978). *Acta Cryst.* A**31**, S358.
HÖFER, H. H., EYSEL, W. & VON ALPEN, U. (1981). *J. Solid State Chem.* **36**, 365-370.
International Tables for X-ray Crystallography (1974). Vol. IV. Section 2.2. Birmingham: Kynoch Press.
IWAI, S., SAKAI, K. & WATANABE, T. (1973). *Kotai Butsuri*, **8**, 43-48.
KEESTER, K. L., EYSEL, W. & HAHN, TH. (1975). *Acta Cryst.* A**31**, S79.
KOBAYASHI, K. & SAITO, Y. (1982). *Thermochim. Acta*, **53**, 299-307.
MEHROTRA, B. N. (1973). *Structures and Phase Relations of Alkali Sulfates, Selanates, Chromates and Carbonates* (in German). PhD Thesis, Technische Hochschule Aachen, Federal Republic of Germany.
MEHROTRA, B. N., HAHN, TH., EYSEL, W. & ARNOLD, H. (1984). In preparation.
MIYAKE, M., MORIKAWA, H. & IWAI, S. (1980). *Acta Cryst.* B**36**, 532-536.
MÜLLER, H. (1910). *Neues Jahrb. Mineral. Geol. Palaeontol.* **30**, 1-54.
PERRIER, C. & BELLANCA, A. (1940). *Period. Mineral.* **11**, 163-300.
SCHUBERT, H. & EYSEL, W. (1980). *Proceedings of the Sixth International Conference on Thermal Analysis*, pp. 93-98. Basel: Birkhäuser.
STEWART, J. M., KRUGER, G. J., AMMON, H. L., DICKINSON, C. W. & HALL, S. R. (1972). The *XRAY72* system-version of June 1972. Tech. Rep. TR-192. Computer Science Center, Univ. of Maryland, College Park, Maryland.

Acta Cryst. (1985). B**41**, 11-21

Investigation of Superlattices in K_xWO_3 in Relation to Electric Transport Properties

BY H. BRIGITTE KRAUSE

Physics Department, Northern Illinois University, DeKalb, IL 60115, *USA*

AND WILLIAM G. MOULTON AND R. C. MORRIS

Physics Department, Florida State University, Tallahassee, FL 32306, *USA*

(*Received* 23 *June* 1983; *accepted* 9 *August* 1984)

Abstract

Single crystals of K_xWO_3 were investigated with electron microscopy and X-ray diffraction methods. In most cases deviations from the hexagonal tungsten bronze structure in terms of commensurate and apparently incommensurate superlattices were observed. The commensurate superlattices in the a-b plane of the hexagonal lattice were, for most compounds, relatively simple, resulting in either an orthohexagonal unit cell or a hexagonal unit cell with two or four times the volume of the tungsten bronze structure, respectively. The 'incommensurate' superlattice rows in the **c** direction indicated a periodicity of 50 to 250 Å or more, depending in part on the crystal composition and temperature. Several different superlattice phases were observed. The superlattice formation is believed to be caused by ordering of the potassium atoms within the channels of the tungsten bronze structure. The data are consistent

0108-7681/85/010011-11$01.50